Contribution from the Chemistry Department and the Energy and Mineral Resources Institute, Iowa State University, Ames, Iowa 50011

Crystal Structures of Tetrakis(μ-formato)dimolybdenum(II)-Potassium Chloride and Two New Polymorphs of Tetrakis(μ-formato)dimolybdenum(II). Single-Crystal Optical Absorption Spectra for Systems with the Molybdenum(II) Formate Dimers

GARY A. ROBBINS and DON S. MARTIN*

Received September 1, 1983

$Mo_2(O_2CH)_4$·KCl was synthesized, and its crystal structure determination indicates a $P\bar{1}$ unit cell with $a:b:c$ = 8.253 (3):10.684 (3):6.769 (3) Å, $\alpha:\beta:\gamma$ = 89.52 (5):109.73 (4):87.03 (6)°, and Z = 2. The two $Mo_2(O_2CH)_4$ molecules occupy inversion centers and are not crystallographically identical. The structure consists of zigzag $Mo_2(O_2CH)_4$-Cl^- chains along a cell diagonal. K^+ ions pack with an 8-fold coordination of five O's and three Cl^-'s. The single-crystal-polarized spectra for the first electronic band of a $1\bar{1}0$ face at 6 K consisted of a single vibrational progression with low resolution based on a 0-0 line at 21 740 cm^{-1} and a $\Delta\bar{\nu}$ of 396 cm^{-1}. A structure determination of a new polymorphic phase, designated as β-$Mo_2(O_2CH)_4$, was found to have a $P2_1/c$ cell with $a:b:c$ = 5.485 (1):12.365 (2):19.862 (4) Å, β = 90.24°, and Z = 6. There are two sets of molecules not crystallographically identical, a 2-fold set occupying special positions with $\bar{1}$ symmetry and a 4-fold set occupying general positions with no symmetry. Single-crystal spectra of a $0\bar{1}3$ face at 6 K showed two sets of highly resolved vibrational progressions separated by 20-30 cm^{-1}. The sets contained progressions based on 0-0 lines at 21 960 and 21 980 cm^{-1} and strong vibronic progressions based on 380- and 750-cm^{-1} vibrations as well. The average separation in the progressions amounted to 355 cm^{-1}. The structure of a third polymorph, γ-$Mo_2(O_2CH)_4$, prepared by sublimation of α-$Mo_2(O_2CH)_4$ had a $P2_1/a$ cell with $a:b:c$ = 7.939 (1):11.193 (1):5.5271 (9) Å, β = 110.86°, and Z = 2. Partial spectra of the first electronic band indicated highly resolved vibrational progressions with a 0-0 line at 22 050 cm^{-1}. The differences in the packing of $Mo_2(O_2CH)_4$ molecules in the various crystals and the perturbation of crystal fields upon the transition moments are discussed.

Introduction

The preparation and crystal structure of tetrakis(μ-formato)dimolybdenum(II) was reported by Cotton et al.[1] with an orthorhombic space group whose parameters are included in Table I. Single-crystal polarized absorption spectra were reported for the 010 face of one of these crystals at 15 K.[2] The low-temperature specta possessed very sharply resolved vibrational components. The strongest progression was based on origins of 21 870 (a) and 21 880 cm^{-1} (c) with no observable absorption below these lines.

Two other moderately intense progressions based on higher origins were discernible in the spectra, and a number of weak progressions were present also. On the basis of the polarization ratios observed for these spectra, it was originally proposed that the first observed absorption band, which has a maximum at 23 400 cm^{-1}, was not the spin-allowed $\delta \rightarrow \delta^*$ transition. Such a transition, $^1A_{1g} \rightarrow {}^1A_{2u}$ ($b_{2g} \rightarrow b^*_{1u}$) under D_{4h} point group molecular symmetry, would be electric dipole allowed for polarization along the z axis, the metal-metal bond. Subsequently, in spectral studies of other carboxylato-bridged dimers involving acetate and trifluoroacetate it was shown that the transition was likely the $\delta \rightarrow \delta^*$ transition, but in the reduced site symmetry of the crystal environment, the transition moment was rotated away from the metal-metal bond.[3,4]

The present work has derived from attempts to prepare higher quality crystals of $Mo_2(O_2CH)_4$ for absorption spectroscopy. This has resulted in the preparation of the double compound $Mo_2(O_2CH)_4$·KCl and two different monoclinic forms of $Mo_2(O_2CH)_4$, which have been characterized by X-ray diffraction structure determinations. Each of the forms possesses a distinctive crystal absorption spectra. Indeed, the low-temperature spectra provided the easiest demonstration of different crystalline phases for very similar appearing preparations. The differences in the crystal spectra are induced by the differing molecular environments of $Mo_2(O_2CH)_4$ in the various crystals.

Table I. Crystallographic Parameters for the $Mo_2(O_2CH)_4$ Polymorphs and for $Mo_2(O_2CH)_4$·KCl

	α-$Mo_2(O_2CH)_4$[a]	β-$Mo_2(O_2CH)_4$	γ-$Mo_2(O_2CH)_4$	$Mo_2(O_2CH)_4$·KCl
space group	$P2_12_12_1$	$P2_1/c$	$P2_1/a$	$P\bar{1}$
cryst syst	orthorhombic	monoclinic	monoclinic	triclinic
a, Å	12.288 (4)	5.485 (1)	7.939 (1)	8.253 (3)
b, Å	12.930 (5)	12.365 (2)	11.193 (1)	10.684 (3)
c, Å	5.500 (1)	19.862 (4)	5.5271 (9)	6.769 (3)
α, deg	90.0	90.0	90	89.52 (5)
β, deg	90.0	90.24 (2)	110.86 (2)	109.73 (4)
γ, deg	90.0	90.0	90.0	87.03 (6)
V, Å^3	872.9 (5)	1347.1 (5)	458.9 (1)	560.8 (3)
Z	4	6	2	2
V/Z, Å^3/molecule	218.2	224.5	229.5	280.4
R	0.063	0.049	0.032	0.055
R_w	0.071	0.059	0.041	0.070
site sym	4-1	2-1, 4-1	2-1	2-1[b]

[a] Reference 1. [b] Molecules are crystallographically independent.

Experimental Section

Preparation of $Mo_2(O_2CH)_4$·KCl. Nitrogen was bubbled through 20 mL of 90% formic acid in a test tube. To this test tube was added 0.178 g of freshly prepared $K_4Mo_2Cl_8·2H_2O$ made by the method of Brencic and Cotton.[5] After 5 min the red solution became a clear yellow color. The system was kept under a nitrogen flow for 3 days as the volume was reduced to 5 mL and some yellow solid material had formed. The product was suction filtered, washed with hexane, and dried in a vacuum desiccator for 10 h. Although much of the solid was very finely divided, a microscopic examination disclosed a number of crystals as thick needles, suitable for X-ray diffraction, and some thin platelike forms that could serve for absorption spectroscopy. When the crystal spectra (see below) proved to be different from that of the orthorhombic $Mo_2(O_2CH)_4$ (designated now the α form), an X-ray structure characterization was undertaken that indicated the formulation as $Mo_2(O_2CH)_4$·KCl.

Preparation of β-$Mo_2(O_2CH)_4$. This polymorph was prepared in attempted recrystallization of $Mo_2(O_2CH)_4$ from samples of $Mo_2(O_2CH)_4$·KCl. $Mo_2(O_2CH)_4$·KCl was dissolved in the 90% formic

(1) Cotton, F. A.; Norman, J. G., Jr.; Stults, B. R.; Webb, T. R. *J. Coord. Chem.* **1976**, *5*, 217.
(2) Cotton, F. A.; Martin, D. S.; Fanwick, P. E.; Peters, T. J.; Webb, T. R. *J. Am. Chem. Soc.* **1976**, *98*, 4681.
(3) Martin, D. S.; Newman, R. A.; Fanwick, P. E. *Inorg. Chem.* **1979**, *18*, 2511.
(4) Martin, D. S.; Newman, R. A.; Fanwick, P. E. *Inorg. Chem.* **1982**, *21*, 3400.
(5) Brencic, J. V.; Cotton, F. A. *Inorg. Chem.* **1970**, *9*, 351.

0020-1669/84/1323-2086$01.50/0

acid, and the volume was reduced under an N_2 atmosphere over a period of several days at room temperature. The yellow crystals were suction filtered, washed with hexane, and dried in the vacuum desiccator. Crystals had the form of plates or short needles. The crystal spectra at 5 K were distinctly different from those of the orthorhombic $Mo_2(O_2CH)_4$. In particular, the vibrational lines in the first electronic band were clearly doubled at slightly different wavelengths from those of the α form. So, a crystal of this preparation was mounted for X-ray diffraction. This crystal proved to have monoclinic axes. The complete crystal structure was determined, and this form has been designated β-$Mo_2(O_2CH)_4$.

Preparation of γ-$Mo_2(O_2CH)_4$. Since samples of the orthorhombic α-$Mo_2(O_2CH)_4$ deteriorate slowly in air and develop a greenish tint, such a sample a was sublimed from a boat in a tube furnace at 270 °C under a slow N_2 flow over a period of 3 h. A crop of yellow crystals consisting of large needles or thin bladelike plates was collected on a cold finger. Three types of crystals could be characterized by their low-temperature single-crystal-polarized spectra. Group I was identified as the α form. Group II contained some very thin, large bladelike plates, ideal for spectroscopy, but too thin for X-ray diffraction. Group III possessed crystal spectra distinctly different from the other two groups and from β-$Mo_2(O_2CH)_4$. A crystal, mounted for X-ray diffraction, possessed a set of monoclinic axes, different from the β form. Its crystal structure, which was solved, describes the third form or γ-$Mo_2(O_2CH)_4$.

X-ray Diffraction Methods. In addition to the complete crystal structure determinations, X-ray diffraction was utilized routinely to confirm the identity of a crystal, to determine the Miller indices for a face examined spectroscopically, and to relate the crystallographic axes with some identifiable macroscopic feature such as the edge of a crystal. Sometimes, actual spectroscopic crystals could be mounted for indexing. The crystal was cemented to a glass fiber by epoxy and mounted on the goniometer head of a four-circle diffractometer that had been constructed in the Ames Laboratory, DOE. The diffractometer was controlled by a PDP-15 computer. Automatic indexing was accomplished on the basis of a set of 10 or more reflections by an interactive program, ALICE, developed by Jacobson.[6] When a sufficiently accurate set of unit cell parameters were available, a number of reflecting planes with small Miller indices were called into the diffracting position and the actual spectroscopic face was identified by careful observation of the orientation of the crystal in each setting. Also, when photographs were taken for oscillation about the three crystal axes, the orientation of the crystal for these photographs provided the location of the axes with respect to the crystal features. For indexing and X-ray diffraction data collection, graphite-monochromated Mo Kα X radiation with λ = 0.709 54 Å was used. A scanning rate of 0.5 s/step of 0.01° in Ω was employed. Data were collected within a 2θ sphere of 50°. As a check on electronic and crystal stability, three standard reflections were remeasured every 75 reflections. The intensities of the standards did not vary significantly through the data collections. The intensity data were corrected for Lorentz polarization, but no absorption corrections were applied. Scattering factors used for non-hydrogen atoms were those of Hanson et al.[7] for $Mo_2(O_2CH)_4$·KCl and β-$Mo_2(O_2CH)_4$. Scattering factors from ref 8 were used for γ-$Mo_2(O_2CH)_4$. The hydrogen atom scattering factors were those of Stewart et al.[9] Estimated deviations in the observed structure factors, F_o, were calculated by the finite-difference method.[10] The discrepancy factors were taken as

$$R = \sum||F_o| - |F_c||/\sum|F_o| \quad (1)$$

$$R_w = (\sum w(|F_o| - |F_c|)^2/\sum w|F_o|^2)^{1/2} \quad (2)$$

where F_c was the calculated structure factor and $w = 1/\sigma^2(F_o)$ with $\sigma(F_o)$ representing the estimated standard deviation in F_o. Refined lattice parameters were computed from separately tuned values of $\pm 2\theta$ for 12–15 reflections by means of the program LATT.[11]

Locations of all Mo atoms were found by Patterson superposition techniques. A series of electron density maps provided locations, and subsequent block-diagonal least-squares refinements of all non-hydrogen atoms with anisotropic thermal parameters were performed. Positional parameters and anisotropic thermal prameters were subjected to a final full-matrix least-squares refinement. For $Mo_2(O_2CH)_4$·KCl, the hydrogen atoms were put at idealized positions and not refined. Electron density difference maps indicated density in the vicinity of these atoms and no other unaccounted density. For the β- and γ-$Mo_2(O_2CH)_4$ structures the hydrogen positions were refined with constant isotropic thermal parameters. The observed and calculated values of the structure factors, thermal parameters, and unrefined calculated hydrogen positions have been deposited as supplementary material. Plots depicting molecular structures and packing were drawn by the ORTEP program.[12]

The crystallographic lattice parameters for $Mo_2(O_2CH)_4$·KCl and β- and γ-$Mo_2(O_2CH)_4$ are collected together with those of α-$Mo_2(O_2CH)_4$ from Cotton et al.[1] in Table I.

Spectroscopic Measurements. The equipment and procedures for recording the polarized crystal spectra have been described previously.[13,14] The spectra with the highly resolved vibrational features were recorded with slit settings that provided a dispersion of no more than 0.12 nm. Plots for the highly resolved spectra were recorded from digital output each 0.1 nm with a scan speed of 0.05 nm/s.

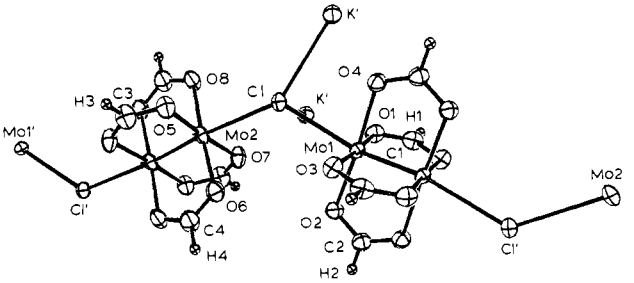

Figure 1. ORTEP perspective drawing of $Mo_2(O_2CH)_4$·KCl.

Table II. Final Non-Hydrogen Atom Positional Parameters and Their Estimated Standard Deviations for $Mo_2(O_2CH)_4$·KCl

atom	x	y	z
Mo(1)	0.39467 (7)	0.44525 (5)	0.42609 (8)
Mo(2)	0.01116 (8)	0.09091 (5)	0.05947 (9)
K	0.1136 (2)	0.4039 (2)	−0.2092 (3)
Cl	0.0735 (2)	0.3341 (2)	0.2412 (3)
O(1)	0.3515 (6)	0.5364 (5)	0.1303 (7)
O(2)	0.5528 (6)	0.3035 (5)	0.3580 (7)
O(3)	0.4252 (6)	0.3476 (5)	0.7121 (8)
O(4)	0.2220 (6)	0.5826 (5)	0.4906 (8)
O(5)	−0.1164 (7)	0.0466 (5)	0.2734 (8)
O(6)	0.2577 (7)	0.0371 (5)	0.2835 (8)
O(7)	0.1342 (7)	0.1494 (5)	−0.1538 (8)
O(8)	−0.2307 (7)	0.1546 (5)	−0.1596 (9)
C(1)	0.449 (1)	0.6244 (7)	0.130 (1)
C(2)	0.7137 (9)	0.3205 (7)	0.421 (1)
C(3)	−0.160 (1)	−0.0658 (8)	0.275 (1)
C(4)	0.311 (1)	−0.0744 (8)	0.283 (1)

Results and Discussion

Structure of $Mo_2(O_2CH)_4$·KCl. For a 0.26 × 0.19 × 0.08 mm crystal, data were collected for four octants. Of the 2460 reflections, 2254 were considered observed ($|F_o| > 3\sigma(F_o)$), and from these 1803 independent reflections were obtained. On the basis of the Howells, Phillips, and Rogers test for a center of symmetry[15] the space group was taken as $P\bar{1}$. Electron density peaks were present in the electron density map

(6) Jacobson, R. A. "An Algorithm for Automatic Indexing and Bravais Lattice Selection: The Programs BLIND and ALICE", Ames Laboratory-USAEC Report IS-3469; Iowa State University: Ames, IA, 1974.
(7) Hanson, H. P.; Herman, F.; Lea, J. D.; Skillman, S. *Acta Crystallogr.* **1960**, *17*, 1040.
(8) Templeton, D. H. "International Tables for X-ray Crystallography"; Kynoch Press: Birmingham, England, 1962; Vol. III, Table 3.3.2C, pp 215, 216.
(9) Stewart, R. F.; Davidson, E. R.; Simpson, W. T. *J. Chem. Phys.* **1965**, *42*, 3175.
(10) Lawton, S. L.; Jacobson, R. A. *Inorg. Chem.* **1968**, 7, 2124.
(11) Takusagawa, F., unpublished work.
(12) Johnson, C. K. USAEC Report ORNL-3794; Oak Ridge National Laboratory: Oak Ridge, TN, March 1971 (second revision).
(13) Martin, D. S. *Inorg. Chim. Acta Rev.* **1971**, *5*, 107.
(14) Fanwick, P. E.; Martin, D. S.; Webb, T. R.; Robbins, G. A.; Newman, R. A. *Inorg. Chem.* **1978**, *17*, 2723.
(15) Howells, E. R.; Phillips, D. C.; Rogers, D. *Acta Crsytallogr.* **1950**, *3*, 210.

Table III. Interatomic Distances and Angles for $Mo_2(O_2CH)_4 \cdot KCl$

Distances, Å			
Mo(1)-Mo(1)′	2.109 (2)	O(1)-C(1)	1.27 (1)
Mo(2)-Mo(2)′	2.102 (2)	O(2)-C(2)	1.274 (9)
Mo(1)-Cl	2.848 (2)	O(3)-C(1)′	1.265 (8)
Mo(2)-Cl	2.880 (2)	O(4)-C(2)′	1.251 (9)
K-Cl	3.260 (3)	O(5)-C(3)	1.27 (1)
$K\text{-}Cl'_{00\bar{1}}$	3.096 (3)	O(6)-C(4)	1.25 (1)
Mo(1)-O(1)	2.129 (5)	O(7)-C(3)′	1.27 (1)
Mo(1)-O(2)	2.103 (5)	O(8)-C(4)′	1.25 (1)
Mo(1)-O(3)	2.124 (5)	K-O(7)	2.730 (6)
Mo(1)-O(4)	2.142 (5)	$K\text{-}O(4)'_{010}$	2.777 (5)
Mo(2)-O(5)	2.121 (7)	$K\text{-}O(3)_{00\bar{1}}$	2.833 (6)
Mo(2)-O(6)	2.132 (5)	K-O(1)	2.905 (5)
Mo(2)-O(7)	2.132 (7)	$K\text{-}O(4)_{00\bar{1}}$	3.149 (6)
Mo(2)-O(8)	2.119 (5)	$K\text{-}Cl_{00\bar{1}}$	3.708 (3)
Angles, deg			
Mo(1)′-Mo(1)-Cl	169.6 (1)	O(5)-Mo(2)-O(6)	92.0 (2)
Mo(2)′-Mo(2)-Cl	174.94 (7)	O(6)-Mo(2)-O(7)	89.5 (2)
Mo(1)-Cl-Mo(2)	128.42 (8)	O(7)-Mo(2)-O(8)	89.6 (2)
Mo(1)′-Mo(1)-O(1)	91.7 (1)	O(8)-Mo(2)-O(5)	88.6 (2)
Mo(1)′-Mo(1)-O(2)	92.7 (1)	O(1)-Mo(1)′-O(3)	176.6 (3)
Mo(1)′-Mo(1)-O(3)	91.7 (1)	O(2)-Mo(1)′-O(4)	176.8 (3)
Mo(1)′-Mo(1)-O(4)	90.5 (1)	O(5)-Mo(2)-O(7)	175.8 (3)
Mo(2)′-Mo(2)-O(5)	92.0 (2)	O(6)-Mo(2)-O(8)	176.9 (3)
Mo(2)′-Mo(2)-O(6)	90.7 (2)	O(1)-C(1)-O(3)′	123.9 (7)
Mo(2)′-Mo(2)-O(7)	91.8 (2)	O(1)-Mo(1)-O(2)	91.0 (2)
Mo(2)′-Mo(2)-O(8)	92.3 (2)	O(2)-Mo(1)-O(3)	88.8 (2)
Mo(1)-O(1)-C(1)	116.1 (4)	O(3)-Mo(1)-O(4)	90.4 (2)
Mo(1)-O(2)-C(2)	116.2 (5)	O(4)-Mo(1)-O(1)	89.6 (2)
Mo(1)-O(3)-C(1)′	116.4 (5)	O(2)-C(2)-O(4)′	123.7 (7)
Mo(1)-O(4)-C(2)′	116.8 (5)	O(5)-C(3)-O(7)′	124 (1)
Mo(2)-O(5)-C(3)	116.4 (6)	O(6)-C(4)-O(8)′	124.3 (7)
Mo(2)-O(6)-C(4)	116.8 (5)		
Mo(2)-O(7)-C(3)′	115.9 (6)		
Mo(2)-O(8)-C(4)′	115.9 (5)		

that were too small for Mo and too large for oxygen. A consideration of the interpeak distances and the compounds employed in the preparation led to the conclusion that these intermediate peaks could be assigned to potassium and chloride ions. The presence of K and Cl was subsequently demonstrated by electron microprobe analysis. The X-ray diffraction could not effectively distinguish between K^+ and Cl^-. The Cl^- were therefore placed in the positions where they served to bridge the dimeric molecules and the K^+ in the spaces between the molecules. The centers of the metal–metal bond of each of the two molecules in a unit cell lie on inversion centers. However, the two dimers are not related by any symmetry operation, and as such each molecule constitutes an independent site. An ORTEP drawing (Figure 1) illustrates the orientation of the molecules and provides the labeling of the atoms for the atomic positions, which are given in Table II. The important interatomic distances are in Table III. As Figure 1 shows, the structure consists of zigzag chains of alternating $Mo_2(O_2CH)_4$ molecules and Cl^- ions with potassium ions present as counterions. That two different molecules alternate in the chain can be seen in the small differences in the Mo–Mo and the Mo–Cl distances and the Mo–Mo–Cl angles. For molecule 1 these parameters have the values of 2.109 (2) Å, 2.848 Å, and 169.6 (1)°, respectively. For molecule 2 these values are 2.102 (1) Å, 2.880 (2) Å, and 174.94 (7)°. The Mo(1)–Cl–Mo(2) angle is only 128.42 (8)°. Any Mo–Cl bond is relatively weak. For example, the Mo–Cl bonds in the octachlorodimolybdate(II) anion of $K_4(Mo_2Cl_8)\cdot 2H_2O$ are 2.44 and 2.48 Å.[16] However, it is interesting to note that the long Mo–Cl bond is associated with the shorter Mo–Mo bond, in agreement with the concept that stronger terminal bonding to the metal reduces the strength of the metal–metal bond with, however, only small changes in the metal–metal bond lengths.[17] Some other examples with Cl^- bridges occur with the tetrakis(μ-carboxylato) complexes of ruthenium dimers. For $Ru_2(n\text{-}O_2CC_3H_7)_4Cl$ with d^{11} configuration and 1.5 bond order, there are zigzag chains,[18] a Ru–Cl distance of only 2.587 Å, a Ru–Cl–Ru angle of 128.4°, and a Ru–Ru–Cl angle of 175.1°. $Ru_2(O_2CCH_3)_4Cl$ is interesting because structures of two polymorphs have been reported. In one[19] the Ru–Cl bond was 2.57 Å, the Ru–Cl–Ru angle was 127.6°, and the Ru–Ru–Cl angle was 177.0°. For the other[20] the Ru–Ru–Cl chains were strictly linear, a requirement of the symmetry with Ru–Cl = 2.58 Å. A similar linear chain was found for the compound $Ru_2[O_2C(C\text{-}H_3)_3]_4Cl\cdot H_2O$ with Ru–Cl = 2.56 Å.[21]

The potassium ion has eight atoms, three Cl's and five O's, packed around it with distances ranging from 2.730 to 3.708 Å. The differences, and especially the long 3.708-Å $K\text{-}Cl_{00\bar{1}}$ and 3.149-Å $K\text{-}O(4)_{00\bar{1}}$ distances, indicate a rather unsymmetrical coordination figure. However, the $O(4)_{00\bar{1}}\text{–}Cl_{00\bar{1}}$ distance was only 3.23 Å, indicating that these two atoms are in contact. The Muetterties and Guggenberger[22] δ-angle test indicated that the coordination figure is closest to a square antiprism. However, the two approximately square faces are not parallel but form an angle of 18°. The average of the two short K–Cl distances, viz. 3.178 (3) Å, is only slightly larger than the 3.14 Å in KCl.[23] Indeed, the molecular volume of $Mo_2(O_2CH)_4\cdot KCl$, 280.4 Å^3, agrees quite closely with the sum of the volumes in α-$Mo_2(O_2CH)_4$ and KCl, 218.2 + 61.9 = 280.1 Å^3.

The variations of the bond distances and angles in the $Mo_2(O_2CH)_4$ molecules indicate only slight deviations from a D_{4h} molecular symmetry that commonly occur as the carboxylate-bridged molecules are packed in crystals.

β-$Mo_2(O_2CH)_4$. Data were collected for two octants for a crystal fragment 0.3 × 0.1 × 0.6 mm. A total of 2882 reflections were collected from which 2492 independent reflections had $|F_o| > 3\sigma(F_o)$. The Howells, Phillips, and Rogers test[15] indicated a centric cell, and the *b*-oscillation photograph exhibited the mirror symmetry expected for a monoclinic lattice. The measured value of β was 90.24 (2)°, so the deviation from 90° was statistically significant. The absence of the mirror symmetry for the *a*- and *c*-oscillation photographs as well indicated that the structure was not orthorhombic. Systematic extinctions for k odd in $0k0$ and l odd of $h0l$ reflections indicated a $P2_1/c$ space group. There were six molecules in the unit cell that required two different crystallographic sites for the molecules. Two molecules were located in the special positions 0, 0, 0 and 0, $^1/_2$, $^1/_2$ with $\bar{1}$ site symmetry. These positions were labeled site 1. Four molecules were then in general positions, site 2, with no imposed site symmetry. The atomic positions are listed in Table IV. Interatomic distances and bond angles for the molecules in the two sites are presented in Table V. The packing arrangement of the molecules and some systematics in bond distances and angles will be discussed after the γ-$Mo_2(O_2CH)_4$ structure is presented.

γ-$Mo_2(O_2CH)_4$. Data were collected for 1916 reflections in four octants, with 743 independent reflections having $|F_o| > 3\sigma(F_o)$. The Howells, Phillips, and Rogers[15] test indicated a centric cell. A *b*-oscillation photograph showed the mirror

(16) Brencic, M. J.; Cotton, F. A. *Inorg. Chem.* **1969**, *8*, 7.
(17) Cotton, F. A.; Walton, R. A. "Multiple Bonds between Metal Atoms"; Wiley: New York, 1982; Section 3.1.2.
(18) Bennett, M. J.; Caulton, K. G.; Cotton, F. A. *Inorg. Chem.* **1969**, *8*, 1.
(19) Togano, T.; Mukaida, M.; Nomura, T. *Bull. Chem. Soc. Jpn.* **1980**, *53*, 2085.
(20) Martin, D. S.; Newman, R. A.; Vlasnik, L. M. *Inorg. Chem.* **1980**, 19, 3404.
(21) Bino, A.; Cotton, F. A.; Felthouse, T. R. *Inorg. Chem.* **1979**, *18*, 2599.
(22) Muetterties, E. L.; Guggenberger, L. J. *J. Am. Chem. Soc.* **1974**, *96*, 1748.
(23) Wells, A. F. "Structural Inorganic Chemistry", 3rd ed.; Clarendon Press: Oxford, 1962; p 357.

Table IV. Final Positional Parameters and Their Estimated Standard Deviations for β-$Mo_2(O_2CH)_4$

atom	x	y	z
Mo(1)	0.1611 (1)	−0.01997 (4)	0.02551 (3)
Mo(2)	0.2720 (1)	0.05052 (4)	0.34210 (3)
Mo(3)	0.5898 (1)	−0.01654 (4)	0.30189 (3)
O(1)	0.1734 (9)	−0.1737 (4)	−0.0201 (2)
O(2)	0.3727 (8)	0.0459 (4)	−0.0547 (2)
O(3)	0.1694 (9)	0.1309 (4)	0.0743 (3)
O(4)	−0.0276 (9)	−0.0882 (4)	0.1074 (2)
O(5)	0.2370 (9)	0.1562 (4)	0.2593 (3)
O(6)	0.4654 (9)	0.1705 (4)	0.3954 (2)
O(7)	0.295 (1)	−0.0495 (4)	0.4283 (3)
O(8)	0.0554 (9)	−0.0682 (4)	0.2907 (2)
O(9)	0.5755 (9)	0.0841 (4)	0.2166 (2)
O(10)	0.8065 (8)	0.1002 (4)	0.3541 (2)
O(11)	0.6312 (9)	−0.1201 (4)	0.3853 (2)
O(12)	0.3951 (8)	−0.1372 (4)	0.2486 (2)
C(1)	0.002 (2)	−0.1950 (7)	−0.0605 (4)
C(2)	0.258 (1)	0.0856 (6)	0.1038 (4)
C(3)	0.395 (2)	0.1492 (6)	0.2147 (4)
C(4)	0.694 (1)	0.1688 (6)	0.3892 (4)
C(5)	0.475 (2)	−0.1117 (6)	0.4305 (4)
C(6)	0.167 (1)	−0.1373 (6)	0.2553 (4)
H(1)	0.02 (2)	−0.264 (8)	−0.081 (4)
H(2)	0.34 (2)	0.129 (8)	−0.138 (4)
H(3)	0.37 (2)	0.206 (7)	0.173 (4)
H(4)	0.79 (2)	0.236 (7)	0.411 (4)
H(5)	0.47 (2)	−0.162 (7)	0.471 (4)
H(6)	0.05 (2)	−0.205 (7)	0.242 (4)

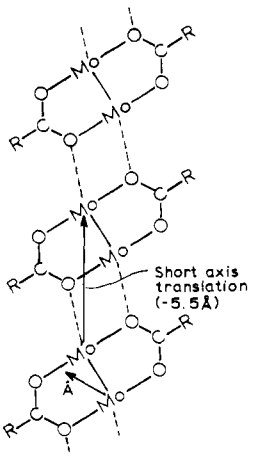

Figure 2. Arrangement of intermolecular bonding common for most crystals of dimolybdenum(II) tetracarboxylates. Two carboxylate rings in each molecule are omitted for clarity.

symmetry of a monoclinic lattice. Systematic extinctions occurred for k odd of $0k0$ reflections and for h odd of $h0l$ reflections so the structure was refined in the $P2_1/a$ space group. There were two molecules per cell which were placed at the $^1/_2$, 0, 0 and $^1/_2$, $^1/_2$, $^1/_2$ positions. The two molecules, related by symmetry, occupy sites with $\bar{1}$ symmetry. Atomic positions are in Table VI, and the interatomic bond distances and the bond angles are in Table VII.

Comparison of the Polymorphic Structures of $Mo_2(O_2CH)_4$. Almost all of the tetrakis(μ-carboxylato)dimolybdenum(II) compounds for which crystal structures are available have a similarity in the intermolecular interactions, which is illustrated in Figure 2. Thus, each molybdenum atom is situated close to one of the carboxylate oxygens on an adjacent molecule. A molybdenum on each adjacent molecule is in turn close to a carboxylate oxygen. The distances are sufficiently close that weak but significant intermolecular bonding interactions must occur. The resulting structure consists of a number of one-dimensional chains of molecules with a series of two-bond linkages between molecules. The molybdenum atoms and the bonding oxygen atoms form a nearly planar array. (In case of inversion centers at the molecular center and between the molecules, the array of intermolecular bonding atoms will be regorously planar.) The crystal translation distance indicated in Figure 2 is about 5.5 Å. All three $Mo_2(O_2CH)_4$ polymorphs have such chain structures. The approximate 5.5-Å translations are c = 5.500 Å for α, a = 5.485 Å for β, and c = 5.527 Å for γ.

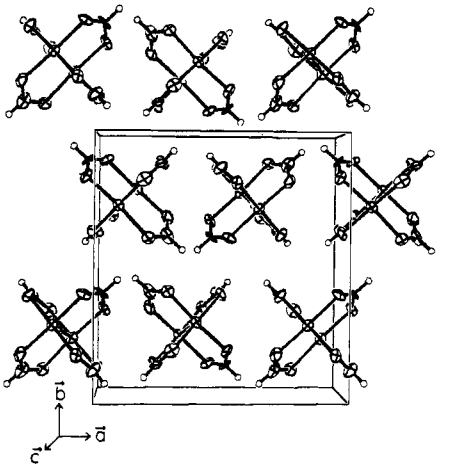

Figure 3. ORTEP drawing of α-$Mo_2(O_2CH)_4$ viewed down the one-dimensional chain direction.

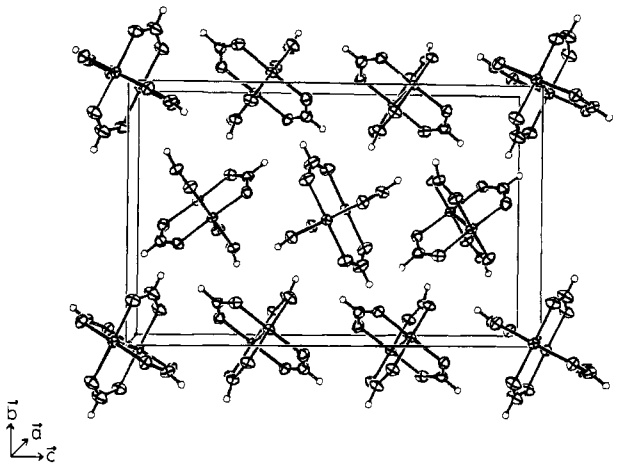

Figure 4. ORTEP drawing of β-$Mo_2(O_2CH)_4$ viewed down the one-dimensional chain direction.

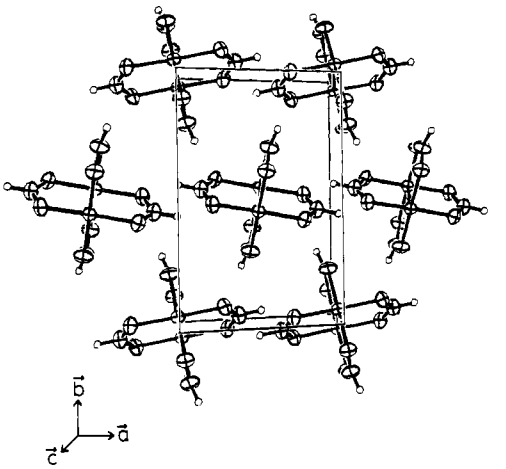

Figure 5. ORTEP drawing of γ-$Mo_2(O_2CH)_4$ viewed down the one-dimensional chain direction.

The linear chains of molecules form rodlike structural units through the crystal. ORTEP perspective drawings of the α-, β-, and γ-$Mo_2(O_2CH)_4$ structures viewed down the chain direc-

Table V. Interatomic Distances and Angles and Their Estimated Standard Deviations for β-$Mo_2(O_2CH)_4$ Molecules

site 1		site 2			
		Distances, Å			
Mo(1)-Mo(1)′	2.093 (1)	Mo(2)-Mo(3)	2.0916 (9)		
Mo(1)-O(2)′(axial)	2.639 (5)	Mo(2)-O(10)(axial)	2.638 (5)	Mo(3)-O(8)(axial)	2.643 (5)
Mo(1)-O(1)	2.107 (5)	Mo(2)-O(5)	2.108 (5)	Mo(3)-O(9)	2.103 (5)
Mo(1)-O(2)	2.136 (5)	Mo(2)-O(6)	2.107 (5)	Mo(3)-O(10)	2.136 (4)
Mo(1)-O(3)	2.102 (5)	Mo(2)-O(7)	2.115 (5)	Mo(3)-O(11)	2.105 (5)
Mo(1)-O(4)	2.109 (5)	Mo(2)-O(8)	2.145 (5)	Mo(3)-O(12)	2.116 (4)
C(1)-O(1)	1.263 (9)	C(3)-O(5)	1.245 (9)	C(5)-O(7)	1.251 (10)
C(1)-O(3)′	1.257 (9)	C(3)-O(9)	1.276 (9)	C(5)-O(11)	1.249 (9)
C(2)-O(2)	1.259 (8)	C(4)-O(6)	1.263 (9)	C(6)-O(8)	1.266 (8)
C(2)-O(4)′	1.265 (10)	C(4)-O(10)	1.259 (8)	C(6)-O(12)	1.259 (8)
C(1)-H(1)	0.95 (9)	C(3)-H(3)	1.10 (9)	C(5)-H(5)	1.02 (9)
C(2)-H(2)	0.96 (9)	C(4)-H(4)	1.07 (9)	C(6)-H(6)	1.07 (9)
		Angles, deg			
Mo(1)′-Mo(1)-O(1)	91.9 (1)	Mo(3)-Mo(2)-O(5)	91.2 (1)	Mo(2)-Mo(3)-O(9)	92.6 (1)
Mo(1)′-Mo(1)-O(2)	90.5 (1)	Mo(3)-Mo(2)-O(6)	93.0 (1)	Mo(2)-Mo(3)-O(10)	90.5 (1)
Mo(1)′-Mo(1)-O(3)	91.7 (1)	Mo(3)-Mo(2)-O(7)	91.7 (1)	Mo(2)-Mo(3)-O(11)	91.6 (1)
Mo(1)′-Mo(1)-O(4)	93.0 (1)	Mo(3)-Mo(2)-O(8)	90.4 (1)	Mo(2)-Mo(3)-O(12)	92.9 (1)
Mo(1)-Mo(1)′-O(2)(axial)	161.9 (1)	Mo(2)-Mo(3)-O(8)(axial)	159.2 (1)	Mo(3)-Mo(2)-O(10)′(axial)	159.3 (1)
Mo(1)-O(2)-Mo(1)′(axial)	108.6 (1)	Mo(2)-O(8)-Mo(3)(axial)	109.2 (1)	Mo(3)-O(10)-Mo(2)(axial)	109.6 (1)
O(1)-Mo(1)-O(2)	90.3 (2)	O(5)-Mo(2)-O(6)	90.0 (2)	O(9)-Mo(3)-O(10)	90.6 (2)
O(2)-Mo(1)-O(3)	89.7 (2)	O(6)-Mo(2)-O(7)	88.7 (2)	O(10)-Mo(3)-O(11)	88.3 (2)
O(3)-Mo(1)-O(4)	90.5 (2)	O(7)-Mo(2)-O(8)	90.9 (2)	O(11)-Mo(3)-O(12)	91.0 (2)
O(4)-Mo(1)-O(1)	89.3 (2)	O(8)-Mo(2)-O(5)	90.2 (2)	O(12)-Mo(3)-O(9)	89.8 (2)
O(1)-Mo(1)-O(3)	176.4 (2)	O(5)-Mo(2)-O(7)	176.8 (2)	O(9)-Mo(3)-O(11)	175.7 (2)
O(2)-Mo(1)-O(4)	176.4 (1)	O(6)-Mo(2)-O(8)	176.5 (2)	O(10)-Mo(3)-O(12)	176.5 (2)
Mo(1)-O(1)-C(1)	115.9 (5)	Mo(2)-O(5)-C(3)	116.8 (5)	Mo(3)-O(9)-C(3)	115.0 (5)
Mo(1)-O(2)-C(2)	117.1 (4)	Mo(2)-O(6)-C(4)	115.9 (4)	Mo(3)-O(10)-C(4)	116.9 (4)
Mo(1)-O(3)-C(1)′	116.4 (5)	Mo(2)-O(7)-C(5)	115.6 (5)	Mo(3)-O(11)-C(5)	116.3 (5)
Mo(1)-O(4)-C(2)′	116.1 (5)	Mo(2)-O(8)-C(6)	117.3 (4)	Mo(3)-O(12)-C(6)	116.6 (5)
O(1)-C(1)-O(3)′	124.1 (7)	O(5)-C(3)-O(9)	124.4 (7)	O(7)-C(5)-O(11)	124.7 (7)
O(2)-C(2)-O(4)′	123.4 (7)	O(6)-C(4)-O(10)	123.7 (6)	O(8)-C(6)-O(12)	122.8 (7)
O(1)-C(1)-H(1)	111 (5)	O(5)-C(3)-H(3)	115 (5)	O(9)-C(3)-H(3)	121 (5)
O(2)-C(2)-H(2)	123 (5)	O(6)-C(4)-H(4)	114 (5)	O(10)-C(4)-H(4)	122 (5)
O(3)′-C(1)-H(1)	124 (5)	O(7)-C(5)-H(5)	113 (5)	O(11)-C(5)-H(5)	122 (5)
O(4)′-C(2)-H(2)	113 (5)	O(8)-C(6)-H(6)	113 (5)	O(12)-C(6)-H(6)	123 (5)

Table VI. Final Positional Parameters and Their Estimated Standard Deviations for γ-$Mo_2(O_2CH)_4$

atom	x	y	z
Mo	0.51056 (6)	0.54768 (4)	0.34326 (7)
O(1)	0.2308 (5)	0.5833 (4)	0.1970 (7)
O(2)	0.4674 (5)	0.3891 (4)	0.1163 (6)
O(3)	0.7899 (5)	0.5172 (4)	0.4667 (8)
O(4)	0.5564 (6)	0.7100 (3)	0.5486 (7)
C(1)	0.1417 (9)	0.5437 (5)	0.328 (1)
C(2)	0.4429 (9)	0.2943 (6)	0.221 (1)
H(1)	0.01 (1)	0.562 (6)	0.26 (2)
H(2)	0.40 (1)	0.227 (7)	0.10 (2)

Table VII. Interatomic Distances and Angles and Their Estimated Standard Deviations for γ-$Mo_2(O_2CH)_4$

	Distances, Å		
Mo′-Mo	2.0910 (8)	O(1)-C(1)	1.261 (7)
Mo-O(1)	2.114 (4)	O(2)-C(2)	1.258 (8)
Mo-O(2)	2.130 (4)	O(3)-C(1)′	1.266 (7)
Mo-O(3)	2.103 (4)	O(4)-C(2)′	1.272 (7)
Mo-O(4)	2.104 (4)	C(1)-H(1)	1.03 (8)
Mo-O(2)′(axial)	2.701 (3)	C(2)-H(2)	0.98 (8)
	Angles, deg		
Mo′-Mo-O(1)	91.7 (1)	Mo-O(1)-C(1)	116.2 (4)
Mo′-Mo-O(2)	91.1 (1)	Mo-O(2)-C(2)	116.8 (4)
Mo′-Mo-O(3)	92.0 (1)	Mo-O(3)-C(1)′	116.4 (4)
Mo′-Mo-O(4)	92.5 (1)	Mo-O(4)-C(2)′	116.5 (4)
Mo′-Mo-O(2)′(axial)	164.45 (9)	O(1)-C(1)-O(3)′	123.7 (6)
Mo-O(2)-Mo′(axial)	109.4 (1)	O(2)-C(2)-O(4)′	123.1 (6)
O(1)-Mo-O(2)	90.3 (2)	O(1)-C(1)-H(1)	117 (5)
O(2)-Mo-O(3)	89.2 (2)	O(2)-C(2)-H(2)	115 (5)
O(3)-Mo-O(4)	90.3 (2)	O(3)′-C(1)-H(1)	120 (5)
O(4)-Mo-O(1)	90.0 (2)	O(4)′-C(2)-H(2)	120 (5)
O(1)-Mo-O(3)	176.3 (2)		
O(2)-Mo-O(4)	176.4 (1)		

tions appear in Figures 3-5. In each structure it is clear that there is approximately a close-packed array of the rodlike units. The principal differences between the structures reside in the relative tilt of the chelate rings in the rods. For each molecule in these figures, one pair of trans chelate rings is viewed nearly edge-on. These are the intermolecular bonding rings. The other rings are tilted somewhat to the viewer. A molecular axis from the center of the metal–metal bond passing through the carboxyl carbon of the tilted rings is approximately normal to the crystallographic stacking axis. This molecular axis will be labeled the y axis. It was rigorously defined by taking the cross products of Mo–Mo bond and the vector between the two O atoms involved in the intermolecular bonding. The z axis was the metal–metal bond, and the x axis ($y \times z$) nearly bisects the chelate rings involved in the intermolecular bonding. In α-$Mo_2(O_2CH)_4$ the y axis of a molecule in a unit cell forms angles of either nearly 0 or 90° with the y axes of different molecules in the cell. For β-$Mo(O_2CH)_4$ the y axis of an individual molecule forms a variety of angles with the y axes of other molecules. With γ-$Mo_2(O_2CH)_4$ there is a single small acute angle between the y axis of the two sites in the cell. The α structure possesses the most efficient packing with a molecular volume of 218.3 Å^3 whereas the β structure has a 2.9% and the γ structure a 5.2% larger molecular volume.

Some details of the intermolecular bonding for the three polymorphs can now be compared. The distances from an Mo atom to the terminal oxygen in α-$Mo_2(O_2CH)_4$ are 2.643 and 2.646 Å, very similar to the three corresponding distances, 2.639, 2.638, and 2.643 Å, observed in β-$Mo_2(O_2CH)_4$. However in γ-$Mo_2(O_2CH)_4$ the distances are significantly longer, 2.701 Å. For α-$Mo_2(O_2CH)_4$ the Mo–Mo···O angle, i.e. the angle between the Mo–Mo bond and the Mo–terminal oxygen bond, is 159.2°, which can be compared to 159.25,

Table VIII. Major Vibrational Lines Resolved in Spectra of α- and β-$Mo_2(O_2CH)_4$ and $Mo_2(O_2CH)_4$·KCl at 6 K

	α-$Mo_2(O_2CH)_4$		β-$Mo_2(O_2CH)_4$ first series		β-$Mo_2(O_2CH)_4$ second series		$Mo_2(O_2CH)_4$·KCl	
line	ν, cm^{-1}	$\Delta\nu$,[a] cm^{-1}	ν, cm^{-1}	$\Delta\nu$,[a] cm^{-1}	ν, cm^{-1}	$\Delta\nu$,[a] cm^{-1}	ν, cm^{-1}	$\Delta\nu$,[a] cm^{-1}
A_0	21 880		21 960		21 980		21 740	
A_1	22 230	350	22 310	350	22 340	360	22 120	380
C_0	22 260	(380)	22 340	(380)	22 370	(390)		
A_2	22 580	350	22 670	360	22 690	350	22 490	370
C_1	22 610	350	22 690	350	22 730	360		
E_0	22 660	(780)	22 730	(770)	22 760	(780)		
A_3	22 930	350	23 030	360	23 050	360	22 860	370
C_2	22 970	360	23 050	360	23 080	350		
E_1	23 000	340	23 080	350	23 110	350		
A_4	23 290	360	unresolved				23 230	370
C_3	23 320	350						
E_2	23 360	360						
A_5	23 610	320					23 590	360
C_3	23 650	330						
E_3	23 710	350						
unresolved	24 080						23 960	370
unresolved							24 310	370
unresolved							24 690	380

[a] Values in parentheses are differences from A_0 and give the origins of vibronic progressions above 0-0. Values without parentheses are differences from the preceding member in the progression.

160.6, and 161.9 in the β form and 164.45° in the γ form. These data imply that the intermolecular bonding in γ-$Mo_2(O_2CH)_4$ is distinctly weaker than in the α and β forms. The deviation of 15–21° from linearity for the Mo′-Mo···O bond occurs despite the fact that Mo would be expected to form its best terminal bond at 180° to the metal–metal bond. This deviation occurs as a compromise with the intermolecular bonding oxygen which with sp^2 hybridization for its σ orbitals would form optimum bonds with 120° between its bonds. In the various polymorphs the Mo–O···Mo angles are as follows: α form, 110.9, 110.6°; β form, 108.6, 109.2, 109.6°; γ form, 106.6°.

Another interesting feature of the intermolecular bonding is indicated by the intramolecular Mo–O bond lengths and Mo–Mo–O angles. In every instance the intramolecular Mo–O bond length for oxygen that forms the intermolecular bond is longer than the average of the Mo–O bonds in the molecule. In only one case of α-$Mo_2(O_2CH)_4$ is it not longer than any other Mo–O bond to an oxygen not involved in intermolecular bonding. (One other bond is 0.003 Å longer in this case.) Also the Mo–Mo–O angle is smaller for the oxygens involved in the intermolecular distances. It appears surprising at first that the oxygen seems to be pushed away from the molybdenum in the adjacent molecule to which it is bonding. However, the oxygen–oxygen distances across the four-membered ring are α = 2.74 (1) Å, β_1 = 2.82 Å, β_2 = 2.79 (1) Å, and γ = 2.92 (1) Å. These distances are sufficiently small that significant repulsions between the oxygens are indicated. The trends in these O–O distances as well as the Mo–Mo–O axial angles appear to give the best indication of the strength of the intermolecular bonds. The ordering of the intermolecular bond strength $\alpha > \beta_2$(general) > β_1(special) > γ appears to be consistent with all the variations in interatomic distances and bond angles. Increases in the intermolecular bonding then results in more effective packing and smaller molecular volumes.

Single-Crystal Spectra. α-$Mo_2(O_2CH)_4$. Single-crystal spectra for the lowest energy band of this polymorph at 15 K were published previously for a 010 face. The lowest energy feature was a single line with a high-energy shoulder. This line, labeled A_0 at 21 880 cm^{-1}, is now believed to be the 0–0 line of a weak $^1A_{1g} \rightarrow {}^1A_{2u}$ transition under D_{4h} symmetry. The crystal lattice of this system $P2_12_12_1$ has four symmetry-related molecules per unit cell so there are four Davydov states. The two observed polarized spectra for *a*- and *c*- polarization apply to transitions to different Davydov states. The difference between the observed A_0 lines in the different polarizations was at most 10 cm^{-1} and no greater than the instrumental uncertainty. Hence, it has been concluded there is no detectable Davydov splitting of these two states. It has been pointed out[4] that the observed polarization ratio $I_\parallel/I_\perp$ for the A_0 line of 0.18 would be provided by a transition moment, shown as A in Figure 2, which lies in the plane of the chelate but oriented 39° away frm the short translation or needle axis ($I_\parallel$ = absorption intensity parallel to the needle axis, here *c* polarization, and $I_\perp$ = intensity perpendicular to the needle axis, here *a* polarization). A Franck–Condon progression based on the O–O line has separations of 350 ± 10 cm^{-1}. Such separations are believed to be based on the A_{1g} metal–metal stretching vibration frequency. Two relatively intense progressions based on origin lines, C_0 and E_0, are at 22 260 and 22 660 cm^{-1}, respectively. The wavenumbers for the observed lines in the A, C, and E progressions in α-$Mo_2(O_2CH)_4$ are listed in Table VIII. Presumably, the C and E progressions are vibronically allowed. Such progressions can be expected to arise from molecular E_g vibrations, which from the C_0 and E_0 lines above the 0–0 origin listed in Table VIII, would have frequencies corresponding to 380 and 780 cm^{-1}, respectively, in the excited $^1A_{2u}$ state. The corresponding spectra of $Mo_2(O_2CCH_3)_4$ and $Mo_2(O_2CCF_3)_4$ also have two relatively intense vibronic progressions. However, the indicated vibrational frequencies are considerably lower for those compounds, amounting to 275 and 260 cm^{-1} for the lower frequency respectively and 545 and 500 cm^{-1} for the higher. The highly resolved structures in the electronic bands indicate that the electronic orbitals involved in the transition must be well shielded from many of the molecular and crystal perturbations that result so frequently in broad unresolved bands for the spectra of coordination compounds. The C and E progressions must correspond to vibrations that involve the metal atoms to possess such high intensities. They likely involve chelate-ring deformations, and their relatively high frequencies indicate that the formate rings are somewhat more rigid than those of acetate and trifluoroacetate.

It may be commented that a number of very weak vibronic lines are observable when spectra are recorded for thick crystals. Polarization ratios of such weak lines are not at all uniform and indicate variously oriented transition dipoles. Similarly inconsistent polarization ratios were also observed for the acetate and trifluoroacetate crystals. Finally it may

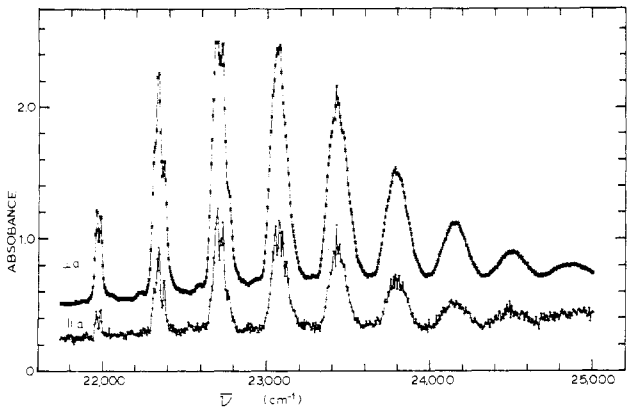

Figure 6. Polarized absorption spectra for a $0\bar{1}3$ face of β-$Mo_2(O_2CH)_4$ at 6 K. The ∥-spectrum is for light polarized in the direction of the needle axis, *a* direction. The thickness of this crystal was 8 ± 1 μm.

be commented that the vibrational structure of the α formate was not as clearly resolved as for the acetate and trifluoroacetate.

β-$Mo_2(O_2CH)_4$. The polarized spectra for a crystal of β-$Mo_2(O_2CH)_4$ are shown in Figure 6. The spectroscopic face was identified as the $0\bar{1}3$ by X-ray diffraction. An examination of the structure presented in Figure 4 shows that this is a high-density face for the crystal and logically can be a well-developed face.

It can be seen immediately from the recorded spectra in Figure 6 that the A_0 line is doubled with a separation of 20–30 cm^{-1}. The lower energy line still lies about 60 cm^{-1} above the A_0 line of the α crystals. The vibrational lines that can be resolved are also included in Table VIII. Insofar as the lines can be resolved, each major line of the α crystal is matched by corresponding lines in the β-crystal spectra that are 90 ± 10 and 110 ± 10 cm^{-1}, respectively, higher energy.

With six molecules per unit cell there will be six different excited crystal states for each molecular transition. The two symmetry-equivalent molecules in the special positions will lead to two Davydov states. With the monoclinic structure the transition moment for attaining one state will be a vector in the *b* direction and the transition moment for reaching the other state will be perpendicular to *b*. For the four symmetry-equivalent molecules in general positions, there will be four Davydov states. However, transitions to two of these states will be optically forbidden. The transition moment for one allowed transition will be a vector parallel to *b* and the other will be perpendicular to *b*. Lines with transition moments parallel to *b* should not be observed in ∥-polarization but will be seen in the ⊥-polarization. The two A_0 lines are seen in both polarizations, and there are no lines seen in ⊥-polarization which are absent in the ∥-spectra. It can be concluded therefore that Davydov splitting is negligible for β-$Mo_2(O_2CH)_4$ and the doubling of the spectra results from the two different crystallographic sites for the molecules.

If the transition moment were directed along the metal–metal bond as expected for a $^1A_{1g} \rightarrow {}^1A_{2u}$ transition in unperturbed D_{4h} symmetry, the polarization ratios are calculated to be $I_\parallel/I_\perp = 7.4$ for the special positions and $I_\parallel/I_\perp = 4.5$ for the general positions. These calculated values are in contrast to the observed values of 0.3 for the two A_0 peaks. If the transition moments in the two sites are placed 39° off the metal–metal bond as shown in Figure 2, the calculated $I_\parallel/I_\perp$ ratios are 0.33 and 0.19, respectively, for the general and special positions, in reasonable agreement with the observed peak ratios. However, the intensities of the lines from the general positions are calculated to be 2–3 times as intense as the lines from the special positions. Since the observed intensities of the lines are nearly equal, the assumptions for the

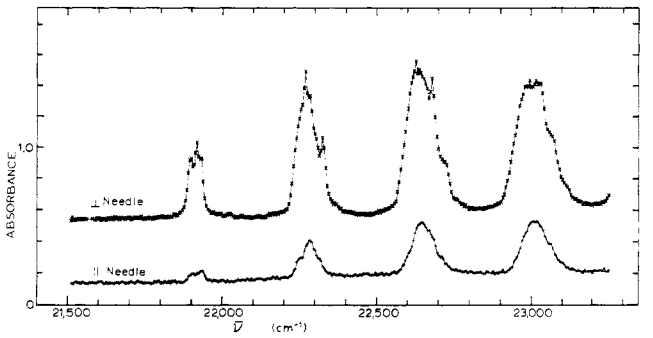

Figure 7. Polarized absorption spectra at 6 K for a thin blade of $Mo_2(O_2CH)_4$, 5 μm thick, prepared by sublimation of α-$Mo_2(O_2CH)_4$. The crystal thickness was 5 ± 1 μm.

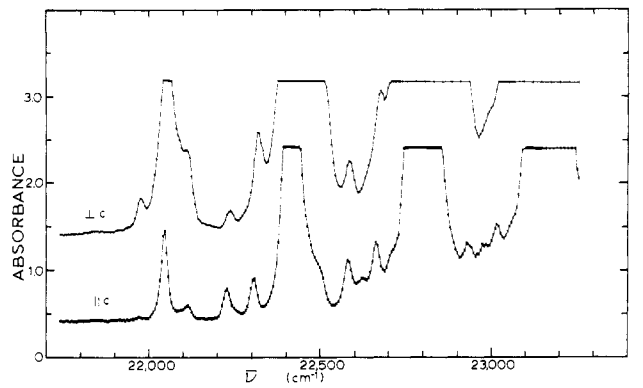

Figure 8. Polarized absorption spectra for a $1\bar{1}0$ face of γ-$Mo_2(O_2CH)_4$ at 6 K. The crystal thickness was 50 ± 10 μm.

calculation, viz. that the different sites have equal transition moments or that the moment vectors lie exactly in the chelate plane, must not be valid. For $Mo_2(O_2CCH_3)_4$ the transition moment lies nearly 10° out of this plane. Unfortunately, since the intensities of the two A_0 lines are so nearly equal, it is not possible to identify the lines for the general and the special positions. From the fact that the structure indicates that the interaction with neighboring molecule for both components decreases from the α to β_2(special) to β_1(general) molecules, the lower energy line at 21 960 cm^{-1} for A_0 is assigned to β_2. However, this assignment is by no means certain.

γ-$Mo_2(O_2CH)_4$. This form was prepared by sublimation of α-$Mo_2(O_2CH)_4$. Originally, it was thought that some sublimed crystals would provide ideal spectroscopic specimens since a number of wide blades, about 0.5 mm wide, 2–3 mm long, and only 5 μm thick, were found that gave uniform extinctions between crossed polarizers. The spectra for one such blade are shown in Figure 7. It can be seen that in the ⊥-polarization there are clearly three peaks of comparable height in the first absorption feature at 21 900–21 940 cm^{-1}. These blades were too thin for satisfactory X-ray diffraction. However, it is believed that this specimen contained at least three stacking patterns with the corresponding site differences.

Figure 8 shows the only spectra obtained for an authentic γ-$Mo_2(O_2CH)_4$ crystal, and it was too thick to provide suitable details of most peaks. The face was identified as the $1\bar{1}0$. However, the A_0 line has occurred at 22 050 cm^{-1}. This is the highest energy observed for this line, apparently because it has the weakest axial bonding. It lies some 160 cm^{-1} above the corresponding line for α-$Mo_2(O_2CH)_4$. The weak vibrational components, rather typical of thick crystal spectra, are clearly evident in Figure 8. It should be noted that there is a weak absorption feature at 21 980 cm^{-1}, below the A_0 line by 70 cm^{-1}. This feature is believed to arise from a very minor component with a stacking arrangement different from the majority of the molecules in the crystal. It appears to be a

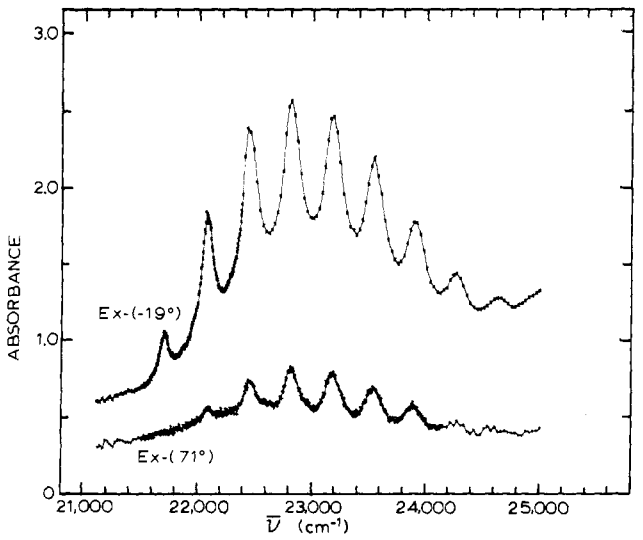

Figure 9. Polarized absorption spectra for a $1\bar{1}0$ face of $Mo_2(O_2CH)_4$·KCl at 6 K.

fairly common occurrence with the molybdenum carboxylates. There was actually a somewhat weaker feature below the A_0' lines of β-$Mo_2(O_2CH)_4$, and similar lines were observed with $Mo_2(O_2CCF_3)_4$. However, we have observed no such component with very thick crystals of α-$Mo_2(O_2CH)_4$ or with $Mo_2(O_2CCH_3)_4$. The variations in the spectra of the various polymorphs of $Mo_2(O_2CH)_4$ provide credence for such assignments to minority components.

$Mo_2(O_2CH)_4$·KCl. Crystals of this compound were typically thin plates rather than the needles formed by $Mo_2(O_2CH)_4$. For a crystal mounted in the X-ray diffractometer, the spectroscopic face was identified as $1\bar{1}0$. One edge of the face was the crystallographic *c* axis. Under crossed polarizers the extinction direction for the high index of refraction lay 71° from the *c* axis (designated Ex-(71°)) between the **c** and the **a** + **b** vectors. The $Mo_2(O_2CH)_4$–Cl^- chains in this structure zigzag about the body diagonal of the cell between 0, 0, 0 and 1, 1, 1. This diagonal lies in the $1\bar{1}0$ face and indeed lies 73.2° from the *c* axis. Hence the Ex-(71°), within about the experimental accuracy, lies along this diagonal. The other extinction is designated as Ex-(−19°). There was no evidence either from the extinctions under crossed polarizers or from polarized spectra for a significant wavelength dependence of the extinction directions such as was observed for the triclinic $Mo_2(O_2CCH_3)_4$.[3]

The single-crystal polarized spectra for the first band of $Mo_2(O_2CH)_4$·KCl at 6 K are shown in Figure 9. In contrast to the $Mo_2(O_2CH)_4$ spectra where the vibrational lines early in the band have widths of a few cm^{-1}, the components of the vibrational structure for the $Mo_2(O_2CH)_4$·KCl spectra have widths of the order of 100 cm^{-1}. Only a single progression in each polarization of Figure 8 is clearly evident, which has been assigned to the A progression. Wavenumbers for the progression are included in Table VIII. The average spacing of the peaks, 370 cm^{-1}, is somewhat higher than for the progressions of $Mo_2(O_2CH)_4$. However, part of this increase could result from the contribution of C and E vibrations, which were not resolved, to the intensities. Spectra of much thicker crystals sometimes contained three or four peaks of a weak progression at lower energy than the progression shown in Figure 9. Such a weak progression is believed to be due to defect sites in the crystal. The crystals for which spectra were reported had somewhat variable thickness, and a thickness therefore cannot be reported.

The intensity for the Ex-(−19°) polarization is much greater than for Ex-(71°). The polarization ratio from the maximum heights of the two bands I(Ex-(−19°))/I(Ex-(71°)) = 5.6. Indeed the first line in the Ex-(71°) polarization is not apparent in the spectra of Figure 8. It was evident in spectra of thicker crystals, however. The metal–metal bond for the molecules at 0, 0, 0 and $^1/_2$, $^1/_2$, $^1/_2$ form angles of 28.0 and 18.3° with Ex-(71°) and 85.5 and 83.4° with Ex-(−19°), respectively. When the intensity contribution of the two sites for transition moments directed along the metal–metal bonds are combined, a polarization ratio I(Ex-(−19°))/I(Ex-(71°)) = ($\cos^2 85.5° + \cos^2 83.4°$)/($\cos^2 28.0° + \cos^2 18.3°$) = 0.011 would be predicted. The serious disagreement between the calculated and observed polarization ratios implies that the crystal field perturbation of the transition moments is even more severe than in crystals of the pure carboxylate dimers. The moments are clearly quite susceptible to the electric field from the ions packed in the low-symmetry structure.

The poor resolution of vibrational structure for $Mo_2(O_2CH)$·KCl indicates that the orbitals involved in the electronic transitions are not as well shielded from perturbations as in the pure carboxylates. The 0–0 transition energy A_0 for $Mo_2(O_2CH)_4$·KCl is significantly lower than for any of the $Mo_2(O_2CH)_4$ polymorphs. This is consistent with a weaker metal–metal bond as a consequence of the stronger terminal bond to the chloride ion, which is also inferred from the longer metal–metal bond.

The formate dimers are the simplest carboxylate dimers of Mo^{II}, and the flexibility they exhibit in crystal packing is perhaps due to the absence of bulky entangling substituents. The highly resolved vibrational structure in the low-temperature crystal spectra provided a sensitive indicator of subtle axial bonding effects for the molecules. They made possible the identification of the new polymorphs and also appear to have value in the indication of minor packing defects in the crystals. The crystal spectra for these carboxylate-bridged dimers emphasize how seriously the crystal site symmetries can perturb the symmetry of the free molecule and how misleading can be the polarization ratios from single-crystal spectra from one compound with low site symmetries. The evidence from all the measured spectra of the molybdenum(II) carboxylates indicates that the first observed electronic transition with highly resolved vibrational structure is a weak but electric dipole allowed $^1A_{1g} \rightarrow {}^1A_{2u}$ in the free D_{4h} molecule.

Acknowledgment. The authors acknowledge Professor R. A. Jacobson for providing assistance and the equipment for X-ray diffraction. Support of the work by NSF Grants CHE 76-83665 and CHE 80-007442 is gratefully acknowledged.

Registry No. $Mo_2(O_2CH)_4$, 51329-49-8; $Mo_2(O_2CH)_4$·KCl, 86750-87-0; $K_4Mo_2Cl_8$, 25448-39-9; Mo, 7439-98-7.

Supplementary Material Available: Tables of calculated H atom positions, anisotropic thermal parameters, and observed and calculated structure factors (18 pages). Ordering information is given on any current masthead page.